

---

# Solving Singular Liouville Equations Using Deep Learning

---

Anonymous Author(s)

Affiliation

Address

email

## Abstract

1 Deep learning has been applied to solving high-dimensional PDEs and successfully  
2 breaks the curse of dimensionality. However, it has barely been applied to finding  
3 singular solutions to certain PDEs, whose boundary conditions are absent and  
4 singular behavior is not a priori known. In this paper, we treat one example of such  
5 equations, the singular Liouville equations, which naturally arise when studying  
6 the celebrated Einstein equation in general relativity by using deep learning. We  
7 introduce a method of jointly training multiple deep neural networks to dynamically  
8 learn the singular behaviors of the solution and successfully capture both the smooth  
9 and singular parts of such equations.

## 10 1 Introduction

11 Most of the mathematical models arising from real world problems, if not all, are governed by  
12 Partial Differential Equations (PDEs). In most cases, closed form solutions to such equations do  
13 not exist. Recently, deep learning has been applied to finding numerical solutions to PDEs and  
14 showed the ability to handle high-dimensional PDEs [5, 4, 13, 11, 7, 2, 1]. However, apart from the  
15 high dimensional problem, the complex nature of PDEs also lies in the fact that their solutions may  
16 admit singularities. For example, the geometric shape of an American football can be described by a  
17 singular solution to Liouville equations. The singularities occur at the two "tips" on the American  
18 football, compared to European footballs where no such tips exist.

19 Deep learning has been barely applied to solving such singular PDEs due to the following reasons.  
20 First, the exact singular behavior of solutions is a priori unknown, such that one deep network model  
21 is not adequate to capture all the information. Moreover, there exists no efficient and satisfactory  
22 way for a neural network to approximate singular functions near singular points, to the best of our  
23 knowledge, despite the fact that smooth function can be approximated by neural networks [3, 6].

24 In this paper, we addressed the above challenges by encoding the different smooth and singular  
25 information of the PDEs into several loss functions and train multiple neural networks to dynamically  
26 learn the behavior of singular solutions near each singularity. More precisely, we treat the singular  
27 Liouville equations which govern metrics of "singular" spheres such as the mentioned American  
28 football. Our neural networks are designed to encode both the smooth and singular parts of the  
29 solutions, while at the same time each neural network is trained to only learn a smooth function. Our  
30 method is inspired by the success of physics-informed neural networks (PINNs) [12, 10, 9], which  
31 have been applied in a wide range of applications. PINNs are appropriate for solving nonlinear PDEs  
32 in the small data setting, which bears similarities to our objective Liouville equations.

33 Main contributions of our work are as follows. To the best of our knowledge, our work is the  
34 first to solve these types of singular PDEs numerically and our method provides a way of solving

35 PDEs whose boundary or initial conditions are present yet not a priori known. Our proposed method  
 36 achieves good accuracy in terms of approximating singular solutions. Moreover, in this work we solve  
 37 the singular Liouville equations on a closed manifold, i.e., a compact manifold without boundary.  
 38 We address the issue that boundary conditions are absent for the PDEs by choosing appropriate  
 39 coordinate charts for the objective manifold. Our work shows the potential of applying deep learning  
 40 method to solving equations numerically on curved manifolds, not only the flat Euclidean space.

41 The motivation to numerically solve singular Liouville equations originated from authors' study on  
 42 deformation of geometric shapes governed by such equations under change of parameters. Thus,  
 43 the numerical results presented in the paper help understand the asymptotic behavior of singular  
 44 manifolds from a differential geometric point of view. Moreover, we expect to extend our method to  
 45 the situation where one deals with singularity of PDEs that exists continuously on divisors, not only  
 46 discretely at points.

## 47 2 Methodology

### 48 2.1 Mathematical Standpoint of the Problem and a Baseline Method

49 We aim to solve the following singular Liouville equation numerically:

$$\begin{aligned} \Delta u + e^{2u} &= 0, \text{ in } \mathbb{R}^2 \setminus \{z_1, \dots, z_m\}, \\ u(z) &= v_i(z) + \log |z - z_i|^{\beta_i - 1}, \text{ for } z \text{ near } z_i, i = 1, \dots, m, \end{aligned} \quad (1)$$

50 where  $\beta_i \in (0, 1)$  are known constants, each  $v_i$  is continuous, and most importantly,  $v_i$  is a priori  
 51 unknown. In other words, solving (1) requires to find both a function  $u$  that satisfies (1) and a family  
 52 of continuous functions  $v_i$  such that the difference of  $u$  and  $v_i$  is a log norm function. The solution  $u$   
 53 can be regarded as having singular asymptotic behavior at marked points  $z_i$ .

54 **Remark 2.1.** *Singular Liouville equation (1) naturally arises as we study the existence of constant*  
 55 *curvature metric on  $\mathbb{S}^2$  that has conical singularities. With the help of differential geometry, one*  
 56 *knows that solution to (1) does exist. However, it is extremely difficult to find the analytical form of*  
 57 *the solution, especially when  $m > 2$ .*

58 We ignore the easiest  $m = 1$  case in (1) since then there does not exist solution to (1) [14]. From now  
 59 on, fix  $m = 2$ . In such case there exists a unique solution to (1). Moreover, in this case the two cone  
 60 angles  $\beta_1$  and  $\beta_2$  must be equal and  $z_1, z_2$  must be the origin and the infinity point in  $\mathbb{R}^2$  respectively.  
 61 More precisely, we can write down the explicit form of the solution to (1) when  $m = 2$ , for some  
 62  $\beta_1 = \beta_2 = \beta$  and  $z_1 = (0, 0), z_2 = \infty$ :

$$u_\beta := \frac{1}{2} \log \frac{4\beta^2 |z|^{2\beta-2}}{(1 + |z|^{2\beta})^2}. \quad (2)$$

63 **Question 2.2.** *Can we solve (1) numerically using deep learning? More precisely, can we recover*  
 64 *the solution (2) by training neural networks to approximately solve (1) when  $m = 2$ ? Due to the*  
 65 *existence of singularities, this is challenging and has not yet been solved numerically.*

66 **A potential solution as the baseline.** The challenge to numerically solve (1) comes from the fact  
 67 that exact singular behavior of solutions is not a priori known and a boundary condition is absent.  
 68 However, when  $m = 2$ , due to the existence of a closed form solution (2), we may use this as a  
 69 priori knowledge and pose a boundary condition for (1). Then we propose two approaches based on  
 70 DeepXDE [8], a library for scientific machine learning and physics-informed learning which requires  
 71 boundary conditions to solve the equation. Treating this method as a baseline, we leave the details of  
 72 theoretical setup and empirical results of these methods to the Appendix. Note that, these methods  
 73 can not be either applied to the general  $m > 2$  case nor used to find unknown singular solutions.  
 74 Besides, empirical evidence implies that our method of training multiple neural networks, which will  
 75 be introduced below outperforms DeepXDE even in this regime.

### 76 2.2 Proposed Method

77 To capture both the smooth and singular information of the solutions to (1), we design and jointly  
 78 train multiple neural networks to numerically solve the singular Liouville equation. More precisely,

79 we aim to approximate both the solution  $u$  to (1) and the a priori unknown continuous functions  $v_i$   
80 for each  $i$ . The advantage is then all the neural networks are used to approximate smooth functions.

81 In more detail, denote by  $w$  the parameters in NNs, we train NNs

$$\mathcal{N}_u(x, y, w), \quad \mathcal{N}_i(x, y, w), \quad i = 1, \dots, m$$

82 so that  $\mathcal{N}_u$  satisfies the first equation in (1),  $\mathcal{N}_i$  approximates each  $v_i$  in (1) and the difference

$$\mathcal{N}_u(x, y, w) - \mathcal{N}_i(x, y, w) \approx \log |x + \sqrt{-1}y - z_i|^{\beta_i - 1}$$

83 prescribes the conical singularities.

84 To encode smooth and singular information into loss functions and construct the corresponding  
85 physics-informed models, we define different loss functions to update the parameters. The loss  
86 function of  $\mathcal{N}_u$  is defined as follows:

$$\ell_u(w) := \frac{1}{N} \cdot \sum_{i=1}^N [\Delta \mathcal{N}_u(x_i, y_i, w) + e^{2\mathcal{N}_u(x_i, y_i, w)}]^2.$$

87 Denote by  $\mathcal{N}_v$  and  $\mathcal{N}_{v'}$ , the NNs to capture conical singularities. The loss function of  $\mathcal{N}_v$  is defined as

$$\ell_v(w) := \frac{1}{M} \sum_{j=1}^M [\mathcal{N}_u(\hat{x}_j, \hat{y}_j, w) - \mathcal{N}_v(\hat{x}_j, \hat{y}_j, w) - \frac{\beta - 1}{2} \log(\hat{x}_j^2 + \hat{y}_j^2)]^2.$$

88 To approximate the singularity at  $\infty$ , we indeed train  $\mathcal{N}_{v'}$  so that

$$\mathcal{N}_u \approx \mathcal{N}_{v'} - (1 + \beta) \log |z|$$

89 for  $z$  restricted to  $\{z \in \mathbb{R}^2 : \delta_1 < |z| < \delta_2\}$ , where  $\delta_1$  and  $\delta_2$  are large. Thus, we sample points  
90 in this region and denote them by  $\{\tilde{x}_s, \tilde{y}_s\}_{1 \leq s \leq M}$ . Then the loss function of  $\mathcal{N}_{v'}$  are defined as  
91 follows:

$$\ell_{v'}(w) := \frac{1}{M} \sum_{s=1}^M [\mathcal{N}_u(\tilde{x}_s, \tilde{y}_s, w) - \mathcal{N}_{v'}(\tilde{x}_s, \tilde{y}_s, w) + \frac{\beta + 1}{2} \log(\tilde{x}_s^2 + \tilde{y}_s^2)]^2.$$

92 In our experiments, we jointly optimize the NNs with the above losses  $\ell_u(w)$ ,  $\ell_v(w)$  and  $\ell_{v'}(w)$ . The  
93 next section introduces our experiment settings and results in detail.

## 94 3 Experiments

### 95 3.1 Experiment Settings

96 **Data sampling:** We first sample  $N$  points from  $C_3 := \{(x, y) \in \mathbb{R}^2 : \sqrt{x^2 + y^2} < 3\}$ . As under  
97 stereographic projection, the area corresponding to  $C_3$  on  $\mathbb{S}^2$  covers 90% of the surface  $\mathbb{S}^2$ . We use  
98  $(x_i, y_i)$ ,  $i = 1, \dots, N$  to denote such data points. Next, we sample  $M$  points close to each prescribed  
99 singular point  $z_i$ ,  $i = 1, \dots, m$ , by taking points from  $C_{\epsilon, i} := \{(x, y) \in \mathbb{R}^2 : |(x, y) - z_i| < \epsilon\}$ .  
100 Usually  $\epsilon$  is set to 0.001. Denote by  $(\hat{x}_j, \hat{y}_j)$ ,  $j = 1, \dots, M$  these data. In experiments, we set  
101  $N = 1000$  and  $M = 1000$ . For the sake of data precision, we avoid having points in  $C_{\epsilon, i}$  that are  
102 too close to  $z_i$ . In our experiments, we avoid points whose distance to the singular point is less than  
103  $0.01\epsilon$ . In practice, since we assume  $m = 2$ , we indeed sample points that are close to  $(0, 0) \in \mathbb{R}^2$  or  
104 close to the infinity point, i.e., restricted to  $\{z \in \mathbb{R}^2 : \delta_1 < |z| < \delta_2\}$  where  $\delta_1$  and  $\delta_2$  are large.

105 **Implementation details:** We train several multilayer perceptrons (MLPs) and denote by  $d = 4$   
106 the number of layers and  $k = 50$  the number of units in each layer. We use the hyperbolic tangent  
107 function  $\tanh(x) := \frac{e^{2x} - 1}{e^{2x} + 1}$ . Note that the ReLU function is not appropriate for the problem since the  
108 second order derivatives of ReLU are trivial and thus it can not be used to approximate the solution to  
109 any second (or higher) order differential equations. In our experiments we find that a combined use  
110 of both first and second order methods gives the best result. In practice we first employ Adam and  
111 then L-BFGS to achieve smallest loss.

112 **Evaluation metrics:** We introduce two different metrics to evaluate the trained model  $\mathcal{N}(w, x, y)$ .  
113 Denote by  $\{(x_i, y_i)\}_{i=1, \dots, N}$  the test data points. The first metric is defined to measure if the model  
114 solves the PDE:

$$\ell_1(w) := \sum_{i=1}^N \frac{1}{N} (\Delta \mathcal{N}(w, x_i, y_i) + e^{2\mathcal{N}(w, x_i, y_i)})^2. \quad (3)$$

115 Another metric is defined to measure if the model coincides with the expected solution  $u_\beta$  as in (2):

$$\ell_2(w) := \sum_{i=1}^N \frac{1}{N} (\mathcal{N}(w, x_i, y_i) - u_\beta(x_i, y_i))^2. \quad (4)$$

116 **3.2 Experiment Results**

117 **Comparison to the ground-truth.** In the training pro-  
 118 cess, we define the total loss to be  $0.4(\ell_v + \ell_{v'}) + 0.2\ell_u$ .  
 119 After training the weighted loss is 0.0114 while  $\ell_u =$   
 120  $0.0133$ ,  $\ell_v = 2.7209e-5$ ,  $\ell_{v'} = 0.0218$ . The test loss  $\ell_1$   
 121 is 0.0134 and  $\ell_2 = 0.4973$ . The heat map of the differ-  
 122 ence between the numerical solution and the real solution  
 123 (2) is shown in Figure 1. We find that close to the origin  
 124 there admits higher error due to the data precision issue  
 125 and singular nature of (2), which are inevitable.

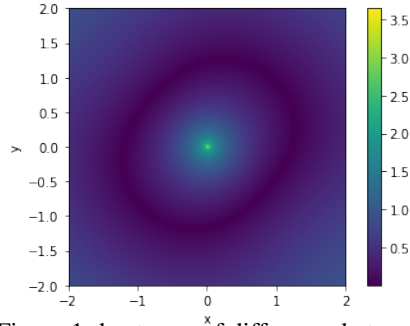


Figure 1: heat map of difference between numerical solution and real solution

126 **Comparison to the baseline method.** A comparison  
 127 between our proposed method and the baseline method,  
 128 which is introduced in the Appendix is shown in Table  
 129 1. By "using prior knowledge" we mean using a priori  
 130 known solution (2) to add boundary conditions to (1). Existence of boundary condition is essential  
 131 for using DeepXDE in the baseline method. The loss functions  $\ell_1$  as in (3) measures if the model  
 132 solves the PDE and  $\ell_2$  as in (4) measures how close the model is to the real solution (2).

| Method                      | Using prior knowledge or not | $\ell_1$ | $\ell_2$ |
|-----------------------------|------------------------------|----------|----------|
| Baseline method (version 1) | Yes                          | 2e-6     | 20.7779  |
| Baseline method (version 2) | Yes                          | 109.9671 | 0.2035   |
| Proposed method             | Yes                          | 4e-7     | 6.6847   |
| Proposed method             | No                           | 0.0134   | 0.4973   |

Table 1: Comparison between different methods in solving singular Liouville equation

133 Table 1 indicates that the baseline method can only capture either the smooth part or the singular part  
 134 of the solution. Indeed, the baseline method tends to learn an almost constant function as the solution  
 135 which is trivial for practical use.

136 In contrast, the proposed method is able to recover singular solutions, even without using a priori  
 137 knowledge. Note that  $\ell_2$  in the last row of Table 1 is an average loss and the main contribution comes  
 138 from test points close to the origin, which reflect the singular nature of (2) and is inevitable to some  
 139 extent considering data precision limit.

140 **Ablation study.** In our proposed method, we could also use a priori knowledge. More precisely,  
 141 one still trains  $\mathcal{N}_u$  to solve (1), and to capture the singularity we only need to train  $\mathcal{N}_v$  such that it  
 142 approximates

$$\mathcal{N}_v \approx u_\beta - (\beta - 1) \log |z|$$

143 given the information from the solution (2).

144 The empirical results are shown in the third row in Table 1. We found that adding a priori knowledge  
 145 does not help learn the singular behaviors of solutions. In other words, our proposed method without  
 146 need of any a priori knowledge is flexible to capture the singularities in the solutions by dynamically  
 147 learning their behaviors near singular points.

148 **4 Conclusion**

149 In this paper we proposed a deep learning method where we design multiple different neural networks  
 150 to solve the singular Liouville equations, which are fully nonlinear, boundary conditions free but  
 151 low-dimensional. Our method, to the best of our knowledge, is the first to treat PDEs that have  
 152 continuous (not a jump) singularities. The proposed model outperforms existing readily available  
 153 PDE solvers that employ deep neural networks when solving singular Liouville equations. The  
 154 numerical solutions to the singular equation are precise enough to reflect the singular nature of the  
 155 objective solution and can be further applied to the study of deformation of specific geometric shapes  
 156 from the theoretical point of view.

157 **References**

- 158 [1] Christian Beck, Sebastian Becker, Philipp Grohs, Nor Jaafari, and Arnulf Jentzen. Solving the  
159 kolmogorov pde by means of deep learning. *Journal of Scientific Computing*, 88(3):1–28, 2021.
- 160 [2] Julius Berner, Markus Dablander, and Philipp Grohs. Numerically solving parametric families  
161 of high-dimensional kolmogorov partial differential equations via deep learning. *Advances in*  
162 *Neural Information Processing Systems*, 33:16615–16627, 2020.
- 163 [3] George Cybenko. Approximation by superpositions of a sigmoidal function. *Mathematics of*  
164 *control, signals and systems*, 2(4):303–314, 1989.
- 165 [4] Weinan E, Jiequn Han, and Arnulf Jentzen. Deep learning-based numerical methods for  
166 high-dimensional parabolic partial differential equations and backward stochastic differential  
167 equations. *Communications in mathematics and statistics*, 5(4):349–380, 2017.
- 168 [5] Jiequn Han, Arnulf Jentzen, and Weinan E. Solving high-dimensional partial differential  
169 equations using deep learning. *Proceedings of the National Academy of Sciences*, 115(34):8505–  
170 8510, 2018.
- 171 [6] Kurt Hornik. Approximation capabilities of multilayer feedforward networks. *Neural networks*,  
172 4(2):251–257, 1991.
- 173 [7] Arnulf Jentzen, Diyora Salimova, and Timo Welti. A proof that deep artificial neural networks  
174 overcome the curse of dimensionality in the numerical approximation of kolmogorov partial  
175 differential equations with constant diffusion and nonlinear drift coefficients. *arXiv preprint*  
176 *arXiv:1809.07321*, 2018.
- 177 [8] Lu Lu, Xuhui Meng, Zhiping Mao, and George Em Karniadakis. Deepxde: A deep learning  
178 library for solving differential equations. *SIAM Review*, 63(1):208–228, 2021.
- 179 [9] M. Raissi, P. Perdikaris, and G.E. Karniadakis. Physics-informed neural networks: A deep  
180 learning framework for solving forward and inverse problems involving nonlinear partial  
181 differential equations. *Journal of Computational Physics*, 378:686–707, 2019.
- 182 [10] Maziar Raissi. Deep hidden physics models: Deep learning of nonlinear partial differential  
183 equations. *The Journal of Machine Learning Research*, 19(1):932–955, 2018.
- 184 [11] Maziar Raissi. Forward-backward stochastic neural networks: Deep learning of high-  
185 dimensional partial differential equations. *arXiv preprint arXiv:1804.07010*, 2018.
- 186 [12] Maziar Raissi, Paris Perdikaris, and George Em Karniadakis. Physics informed deep learn-  
187 ing (part i): Data-driven solutions of nonlinear partial differential equations. *arXiv preprint*  
188 *arXiv:1711.10561*, 2017.
- 189 [13] Justin Sirignano and Konstantinos Spiliopoulos. Dgm: A deep learning algorithm for solving  
190 partial differential equations. *Journal of Computational Physics*, 375:1339–1364, 2018.
- 191 [14] Marc Troyanov. Metrics of constant curvature on a sphere with two conical singularities.  
192 *Differential geometry*, pages 296–306, 1989.

193 **Appendix**

194 In order to use existing package to solve (1), we "cheat" by using a priori known solution (2) to add  
195 boundary condition so that the original PDE is converted to a Dirichlet problem. Then we propose  
196 two approaches based on DeepXDE [8] to solve the new problems.

197 **The first approach:** We solve the following Dirichlet problem:

$$\begin{aligned} \Delta u + e^{2u} &= 0, \quad \text{in } \{z \in \mathbb{R}^2 : \epsilon < |z| < \delta\}, \\ u &= \frac{1}{2} \log \frac{4\beta^2 |z|^{2\beta-2}}{(1 + |z|^{2\beta})^2}, \quad \text{on } \{z \in \mathbb{R}^2 : |z| = \epsilon \text{ or } \delta\} \end{aligned} \quad (5)$$

198 using the package DeepXDE [8].

199 We expect to recover the solution  $u_\beta$  in (2) by solving (5) as we impose small/large enough  $\epsilon$  and  $\delta$ .  
200 We use  $\ell_1$  in (3) and  $\ell_2$  in (4) to test the accuracy of the model after training process.

201 **The second approach:** Instead of solving (1) for  $u$ , under the assumption of  $m = 2$ , we may  
202 reformulate the problem of solving (1) to another PDE for the function  $v_i$ . Indeed, in this case,  
203 globally there holds

$$u = v + \log |z|^{\beta-1}, \quad \text{in } \mathbb{R}^2,$$

204 where  $\beta$  is the cone angle (note that in this case the two cone angles at 0 and  $\infty$  must be the same).  
205 The key point is that  $v$  is a smooth function. To solve  $u$  in (1) it is then enough to solve  $v$ .

206 **Lemma .1.** *When  $m = 2$ , the function  $v$  in (1) satisfies the following PDE:*

$$\Delta v + e^{2v} |z|^{2\beta-2} = 0, \quad \text{in } \mathbb{R}^2. \quad (6)$$

207 *Proof.* From (1), we obtain

$$v = u - (\beta - 1) \log |z|.$$

208 Then taking Laplacian of  $v$ , we get

$$\begin{aligned} \Delta v &= \Delta u - \Delta(\beta - 1) \log |z| \\ &= \Delta u \\ &= -e^{2u}, \quad \text{using (1)} \\ &= -e^{2v} |z|^{2\beta-2}. \end{aligned}$$

209

□

210 Note that the PDE (6) has singularity since  $2\beta - 2 < 0$ . In other words, although  $v$  as a smooth  
211 function has better regularity compared to  $u$ , the PDE for  $v$  has a singular term, which does not  
212 happen for  $u$ .

213 To solve (6) using DeepXDE, we need to modify it to a Dirichlet problem. To achieve this, we solve  
214  $v$  in the unit disk with the needed boundary condition:

$$\begin{aligned} \Delta v + e^{2v} |z|^{2\beta-2} &= 0, \quad \text{in the unit disk,} \\ v &= \log \beta, \quad \text{on the boundary.} \end{aligned} \quad (7)$$

215 We only need to solve  $v$  in the unit disk due to the fact that it is enough to solve  $v$  for the two  
216 hemispheres, while each hemisphere corresponds to the unit disk under stereographic projection. The  
217 boundary condition in (7) comes from the prior knowledge of  $u_\beta$  in (2), which serves as the solution  
218 to (1) when  $m = 2$ .

219 We also use  $\ell_1$  in (3) as the test loss. Besides, for this approach we modify  $\ell_2$  to the average  $L^2$   
220 difference between the model  $\mathcal{N}_v$  and the real solution  $v_\beta$ :

$$\ell_2 = \ell(\mathcal{N}_v, v_\beta) := \frac{1}{N} \sum_{i=1}^N |\mathcal{N}_v(x_i, y_i) - v_\beta(x_i, y_i)|^2,$$

221 for test data set  $\{(x_i, y_i)\}_{1 \leq i \leq N}$ .